Research Report
2009-11

Design and Optimization of a Novel Hybrid Transverse / Longitudinal Flux, Wound-Field Linear Machine for Ocean Wave Energy Conversion

J. Vining, T.A. Lipo, & G. Venkataramanan

Dept. of Elect. & Comp. Engr.
University of Wisconsin-Madison
1415 Engineering Drive
Madison, WI 53706

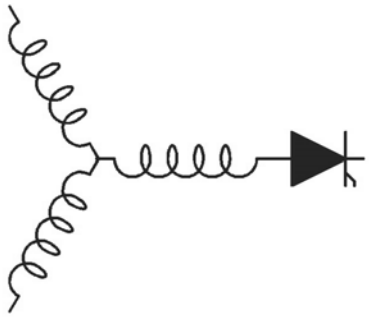

Wisconsin
Electric
Machines &
Power
Electronics
Consortium

University of Wisconsin-Madison
College of Engineering
Wisconsin Power Electronics Research Center
2559D Engineering Hall
1415 Engineering Drive
Madison WI 53706-1691

Design and Optimization of a Novel Hybrid Transverse / Longitudinal Flux, Wound-Field Linear Machine for Ocean Wave Energy Conversion

J. Vining, T.A. Lipo, G. Venkataramanan
Department of Electrical and Computer Engineering
University of Wisconsin - Madison
Madison, WI, USA
vining@wisc.edu, lipo@engr.wisc.edu, giri@engr.wisc.edu

Abstract— **This paper develops an analytical model for a novel double-sided hybrid transverse / longitudinal flux linear machine for use in ocean wave energy converter (WEC) applications. While several machine topologies exist for direct-drive power take-off in buoy-type WECs, the intent of this paper is to introduce a new type of linear machine for possible use as a direct-drive in future WECs. The topology considered consists of a short primary (stator) and a long secondary (translator). The translator is sandwiched between two stators that carry flux in the longitudinal direction, while the translator carries flux in the transverse direction. Operating conditions for WECs require low speeds, yielding machine characteristics such as a large number of coil turns, high inductance, and high force density. Finite element analysis (FEA) is used to optimize and validate analytical results as well as calculate leakage and magnetizing inductance.**

Keywords-ocean wave energy; wound-field linear asynchronous generator; linear machine design; FEA optimization

I. INTRODUCTION

Wave energy converters (WECs) fall into two categories, namely the buoy-type and turbine-type. The linear machine proposed in this paper is meant for use as a direct-drive power take-off in the buoy-type WEC. Current commercial power take-off strategies for the buoy-type involve coupling a hydraulic system to an electric generator. The reliability advantage of electromechanical systems over hydraulic systems is well established among automotive and aerospace applications. In WEC applications, the issue of the hydraulic system's reliability also brings up environmental concerns since toxic hydraulic fluid could contaminate surrounding ocean fauna. Furthermore, coupling hydraulics to an electrical generator adds unnecessary complexity, failure modes, and power loss. To mitigate these problems, a linear generator may be used to remove the hydraulic intermediary.

Several linear machine candidates exist including the permanent magnet machine, switched reluctance machine, and induction machine. Moreover, these come in different varieties such as transverse flux and longitudinal flux. Most research to date has focused on the permanent magnet machine [1]-[4]; however, this machine experiences significant cogging forces at low speeds due to attraction between the high energy permanent magnets and stator teeth [5], [6]. These forces reduce reliability by causing mechanical stresses that shorten the life of the bearings. Some research has been devoted to both the reluctance and induction machines, but their poor performance at low speeds has deemed them unsuitable for WECs [1].

As an alternative to these machines, this paper develops an innovative hybrid transverse / longitudinal flux, wound-field asynchronous linear generator. Similar to the well-established doubly-fed induction generators in wind power applications, this topology allows for control of the translator flux, yielding a higher power factor and increased efficiency compared to a typical induction machine. In general, the hybrid transverse / longitudinal flux design topology has the benefits of the transverse flux machine's increased shear force density while not suffering from its poor magnetic coupling [7]. The main difficulty in creating this design is the inherent low speed of the translator, which reduces machine's *goodness* as defined by Laithwaite [8]. Low speeds also produce machine characteristics such as a large number of coil turns, high inductance, and low power factor.

The contents of this paper are laid out as follows: Section II introduces the machine topology, Section III develops the analytical electromagnetic design, and Section IV presents an FEA validation and optimization of the analytical machine design.

II. HYBRID LINEAR MACHINE DESCRIPTION

Because of the novelty of this field, many of the diverse generator topologies, such as this hybrid machine, have been left unexplored. The topology of the wound-field machine is similar to existing linear induction machines with the exception that coil turns are used instead of copper/aluminum bars in the translator. Another difference from the majority of linear induction machines presented in the literature is that this new machine is double-sided instead of single-sided [9], [10] since symmetrical loading and increased force density can be achieved with multiple sides [11].

Research Report
2009-11

Design and Optimization of a Novel Hybrid Transverse / Longitudinal Flux, Wound-Field Linear Machine for Ocean Wave Energy Conversion

J. Vining, T.A. Lipo, & G. Venkataramanan

Dept. of Elect. & Comp. Engr.
University of Wisconsin-Madison
1415 Engineering Drive
Madison, WI 53706

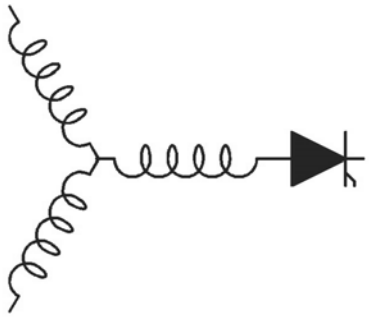

Wisconsin
Electric
Machines &
Power
Electronics
Consortium

University of Wisconsin-Madison
College of Engineering
Wisconsin Power Electronics Research Center
2559D Engineering Hall
1415 Engineering Drive
Madison WI 53706-1691

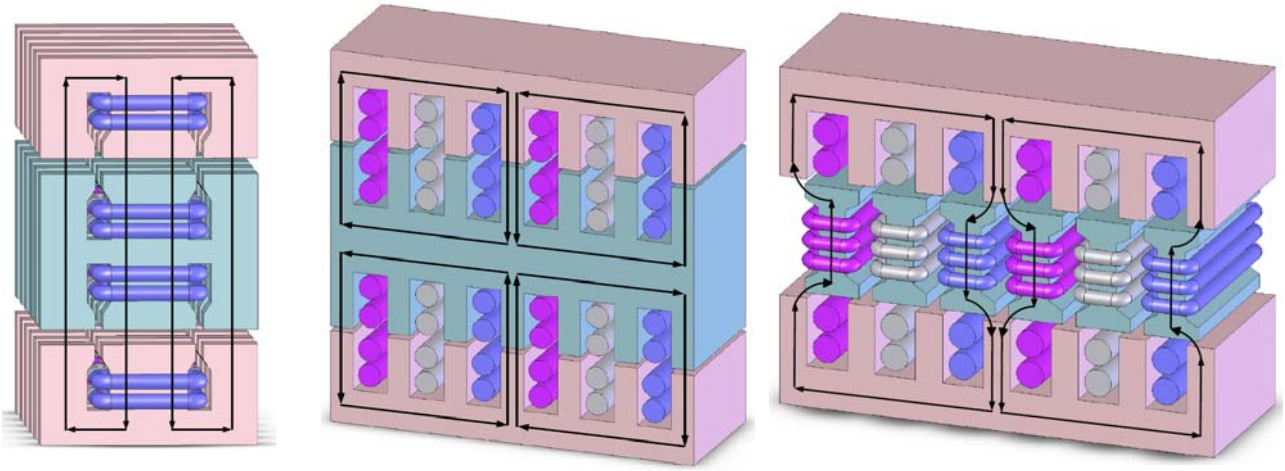

(a) Transverse Flux Linear Machine

(b) Longitudinal Flux Linear Machine

(c) Hybrid Longitudinal / Transverse Flux Linear Machine

Figure 1. Flux Paths for One Pole Pair (qs=1, qr=1) of Three Wound-Field Linear Machines

A. Description of Possible Machine Flux Configurations

Fig. 1 illustrates the topology of the proposed wound-field linear machine in comparison with more classical designs. One pole pair of each linear machine is depicted, where the number of stator and translator slots per pole per phase is the same. Fig. 2 provides a legend for the phases, flux path, and stator / translator components in Fig. 1.

The transverse flux machine and the typical longitudinal flux machine are shown Fig. 1 (a) and Fig. 1 (b) respectively. Combining components of these two machines yields a hybrid machine with a longitudinal flux path in the stator and a transverse flux path in the translator as illustrated in Fig. 1 (c). The machine incorporates beneficial characteristics of both the longitudinal and transverse flux machines in two ways:

- The longitudinal flux path in the stator improves magnetic coupling
- The transverse flux path in the translator increases force density

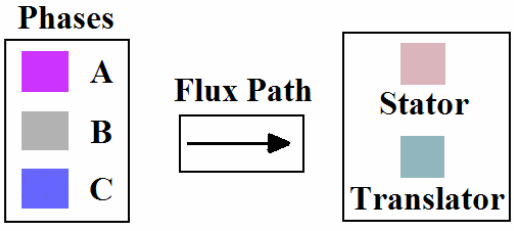

Figure 2. Key to Fig. 1

B. Machine Operating Mode

This machine topology has three possible modes of operation:

1) Synchronous (DC on Translator)
2) Asynchronous (AC on Translator)
3) Short-Circuited Squirrel Cage

The merits of each of these operating modes are listed in Table I. The design in Section III assumes an asynchronous machine; however, the windings on the translator may be excited in synchronous fashion or shorted in a squirrel-cage configuration.

TABLE I. MERITS OF DIFFERENT OPERATING MODES

Asynchronous	*Synchronous*	*Short-Circuit Squirrel Cage*
• In large machines, the asynchronous mode is more stable than the synchronous mode due to damping effects • Offers improved power capture ability over basic induction machines due to slip power recovery, etc. • Requires more power electronics • A flexible power cord can be used instead of slip rings as used in rotary machines	• Fewer power electronics than the asynchronous mode • Windings may be more reliable than permanent magnets in high-g ocean environment since they are less brittle	• Robust design requiring the least amount of power electronics • Poor performance at low speeds • Degree of control is limited

C. Linear Machine Characteristics

In considering linear machine topologies, it is necessary that the active area of energy conversion remains constant as the translator moves. This requires either the stator or the translator to be longer than the other. Since there are two stator sides, a longer translator and shorter stator leads to material savings. This is generally termed short primary, long secondary. Even though the number of translator poles exceeds that of the stator since the translator is longer, the number of overlapping poles always remains the same.

III. Analytical Model: Electromagnetic Design

Whereas typical machine designs are based on a given power, voltage, and current rating, this design starts with given stator dimensions and a desired voltage rating from which the power and current ratings can be deduced. This approach allows the designer to take an off-the-shelf lamination stack and custom design the rest of the machine based on that stator lamination stack. The analytical model is derived using machine theory presented in [12].

The length of the translator is based on the significant wave height in a particular wave climate. If we assume sinusoidal waves, the velocity of the translator is calculated as the derivative of the wave height with the predominant wave period. For coastal U.S. wave climates, the velocity is roughly 0.5-0.7 m/s. From this we can find the rated electrical frequency of the linear machine.

The following numerated process is used in the design of this hybrid machine, where steps 2) and 3) are key design parameters. The choice of design parameter in step 3) is discussed further in Section IV with regards to machine optimization. Fig. 3 contains the physical notation used in key equations (1) - (4).

1) Use continuity of flux through the stator teeth to obtain $B_{g,ave}$ which does not cause saturation
2) Choose the stator and translator coil pitching and distribution in order to calculate the winding factor
3) Pick a ratio between translator pole and slot pitch (r_{ts} = $t_{r,tip}$ / $\tau_{r,slot}$). This is a *key design parameter*.
4) Use continuity of flux between the airgap and the translator core to find $t_{r,core}$
5) Use the stored airgap magnetic energy per pole and the flux linkage per pole to find the number of series turns per phase (there are no parallel circuits in this design because we want higher voltage). This is different than most machines because of the double-sided airgap and winding arrangement in the translator.

$$N_{series} = \frac{\pi}{4}\frac{\sqrt{2}V_{LN,RMS}}{\left(\omega_e k_{h=1} B_{g,1}\right)\left(w\tau_{pole}\right)}. \qquad (1)$$

6) The rated current is found from the given stator slot dimensions and the number of series turns per phase.

$$I_{RMS} = \frac{t_{s,slot} h_{s,slot} J_{RMS} k_{cu}}{2N_{s,coil}}. \qquad (2)$$

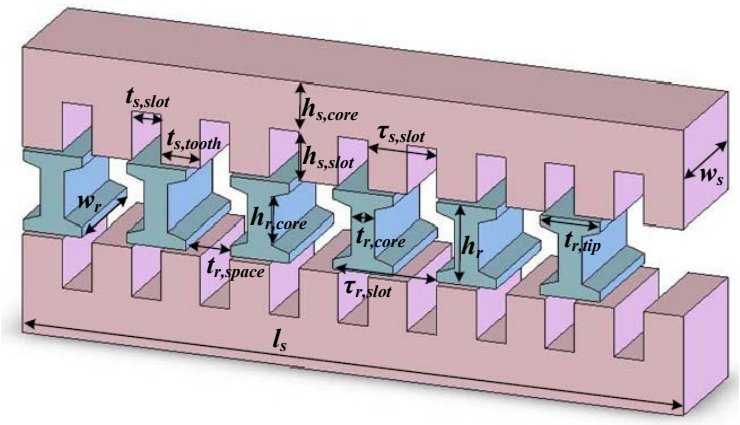

Figure 3. Linear Machine Physical Parameter Notation

7) The rated current gives us the height of the rotor core necessary to contain all the conductors.

$$h_{r,core} = \frac{2I_{RMS}N_{r,coil}}{\frac{1}{2}\left(t_{r,tip} - t_{r,core}\right)J_{RMS}k_{cu}}. \qquad (3)$$

8) Now that we have all the machine dimensions, we can find the MMF of one pole which gives us the magnetizing inductance.

$$L_m = \frac{3}{2}\frac{4}{\pi}\frac{\left(k_{s,h=1}N_{s,series}\right)^2 B_{g,ave}\tau_{s,pole}w_{s,eff}}{P\mathcal{F}_{pole}}. \qquad (4)$$

IV. Finite Element Analysis: Design Validation and Optimization

The FEA tool JMAG is used to validate and optimize the analytical design. To reduce computational complexity, a 2-D representation of two pole pairs is modeled. Further computational reduction comes from exploiting magnetic symmetry through the midsection the translator. There are two principle downsides in using this reduced FEA model. By modeling only two pole pairs, the effect of longitudinal leakage flux at the stator ends is neglected. However, since there are so many poles, this effect is minimal. Another shortcoming is that in a 2-D model, end-winding leakage flux is also neglected. In spite of this, the reduced FEA model is necessary due to the number of iterations needed for the optimization process.

Four candidate machine models (with r_{ts} = 0.6, 0.625, 0.65, and 0.675) are investigated. Each model is run for 25 discrete translator positions over one pole pitch, thus allowing us to detect variations in the ripple force and inductance over one pole pitch.

The four candidate machine models are compared using an optimization process described later in this section. The optimization design criteria and machine parameters for the chosen design are listed in Tables II and III respectively.

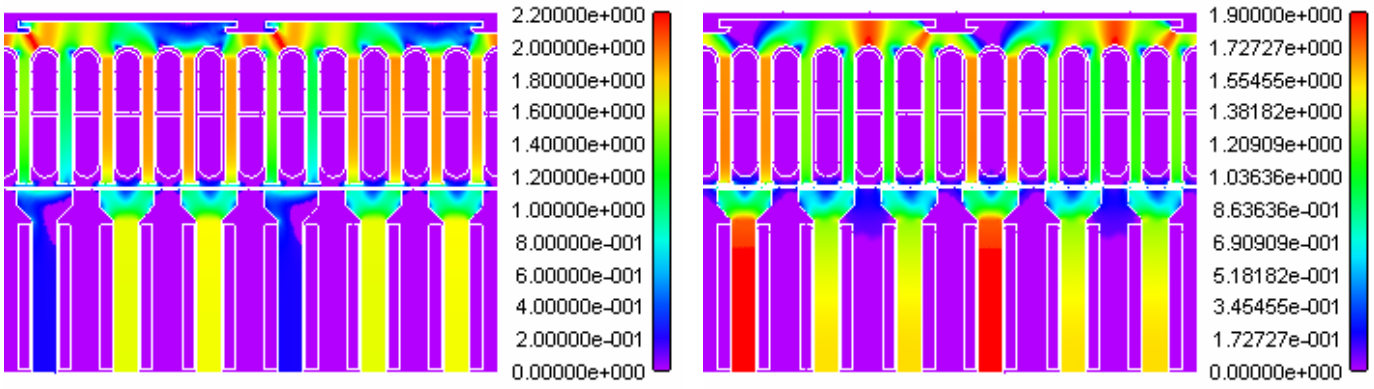

(a) All Stator Phases Excited (b) All Translator Phases Excited

Figure 4. JMAG Screen Shots Showing Magnetic Flux Density for the r_{ts} = 0.675 Model (Units are in T)

A. *Design Validation*

The verification process involves confirming that key analytical design constraints are fulfilled. The following list enumerates key criteria that must be met:

1) The magnetic flux density in the airgap should match the design given the rated current, resistance, and number of coil turns.
2) Neither the stator or translator iron should be saturated.
3) The attractive force between the stator and translator should match theoretical prediction.

The JMAG screen shots in Fig. 4 confirm that the derived current, stator / translator coil turns, and resistance values based on parameters in Table III are correct. As a wound-field asynchronous machine, both the stator and translator are designed to separately produce the rated airgap flux density without experiencing saturation. Here we see that items 1 and 2 of the list are in compliance.

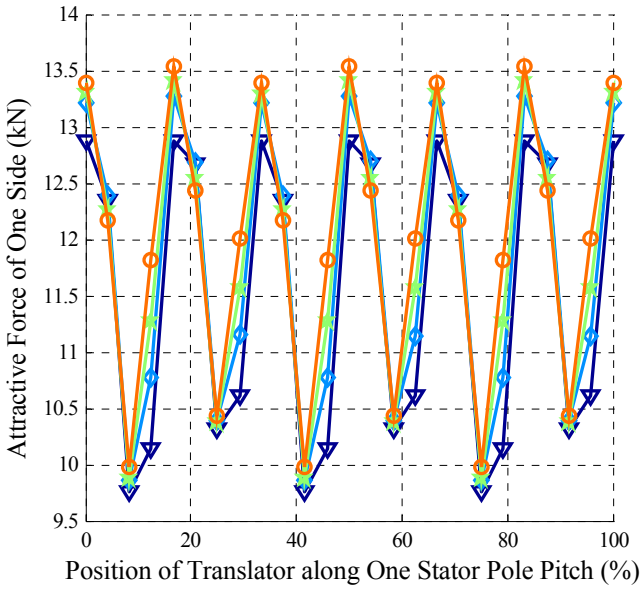

Figure 5. Attractive Force Variation of One Stator Side from FEA

The attractive force is the force component normal to the airgap surface, which may be calculated using

$$F_{\substack{mag \\ attraction}} = \frac{B^2 A_{gap}}{2\mu_o} = 12.63 \text{ kN} \quad (5)$$

for this design case. A plot of the predicted attractive force from FEA as a function of translator position is shown in Fig. 5. It may be observed that the FEA result matches the analytical calculation in (5), thus confirming item 3. Fig. 6 provides the key for Fig. 5 and the rest of the figures in this section.

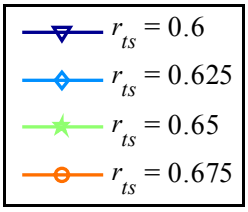

Figure 6. Key to Fig. 5 – Fig. 13

B. *Design Optimization*

Given the four candidate machine models, the goal of the FEA optimization is to find the model whose r_{ts} ratio (see Step 3 of the analytical design process) yields the best magnetic coupling and lowest ripple force. This section first presents inductance and ripple force calculations followed by an analysis of which model gives the best results.

1) *Inductance Calculations and Optimization*

The magnetizing inductance is extracted from JMAG via the following procedure:

1) Excite one phase in JMAG
   i) Stator L_{mag} inductance: Excite one phase of the stator
   ii) Translator L_{mag} inductance: Excite one phase of the translator
2) Find the flux of one MMF loop passing through the airgap. There are two methods to do this:

i) Perform a closed surface integral of the magnetic flux density around one MMF loop

$$\text{Method A:}\quad \Phi_{\substack{mmf\\loop}} = \oiint_{S} B_y \cdot d\vec{S}\,. \tag{6}$$

ii) Perform a closed line integral of the magnetic vector potential around one MMF loop

$$\text{Method B:}\quad \Phi_{\substack{mmf\\loop}} = \oint_{\ell} A_z \cdot d\vec{\ell}\,. \tag{7}$$

3) Find the flux linkage

i) Stator L_{mag}: Multiply the flux density of one MMF loop by the number of *overlapping* poles and the number of coil turns per phase per pole in the translator

$$\Phi_{\substack{s,\\linkage}} = \Phi_{\substack{s,\\mmf\\loop}} N_{\substack{r,\\pole}} P\,. \tag{8}$$

ii) Translator L_{mag}: Multiply the flux density of one MMF loop by the number of *overlapping* poles and the number of coil turns per phase per pole in the stator

$$\Phi_{\substack{r,\\linkage}} = \Phi_{\substack{r,\\mmf\\loop}} N_{\substack{s,\\pole}} P\,. \tag{9}$$

4) Find the magnetizing inductance: Divide the flux linkage by the peak current (i.e. the current applied in the FEA model)

$$L_{\substack{s/r,\\mag}} = \Phi_{\substack{s/r,\\linkage}} \Big/ I_{Peak}\,. \tag{10}$$

The self inductance is calculated much like the magnetizing inductance except that the stator / translator MMF in step 2 is taken from the stator / translator cores respectively. Another difference is that the stator / translator flux linkage in step 3 is found by multiplying by the number of turns in the stator / translator respectively.

The leakage inductance cannot be calculated directly but instead must be found indirectly from the magnetizing and self inductances as shown in equation (11).

$$L_{\substack{s/r,\\leak}} = L_{\substack{s/r,\\self}} - L_{\substack{s/r,\\mag}}\,. \tag{11}$$

Figs. 7 – 10 illustrate the stator / translator magnetizing and leakage inductance profiles for the four r_{ts} models at 25 translator positions spanning one pole pitch. It is apparent that the stator magnetizing inductance is greater than the translator magnetizing inductance, but this is expected given the nature of the transverse flux path in the translator. Conversely, the stator and translator leakage inductances do not differ as much. Another important observation to be made is that the inductance varies periodically with a periodicity equal to one stator slot pitch.

By simply looking at these inductance graphs, it is not easy to deduce which model has the best magnetic coupling. Therefore it is necessary to use a single metric for comparison. In this case, we can use the ratio of magnetizing to leakage inductance as our metric. The model with the highest ratio would then have the best magnetic coupling. Figs. 11 and 12 show these ratios for the stator and translator respectively.

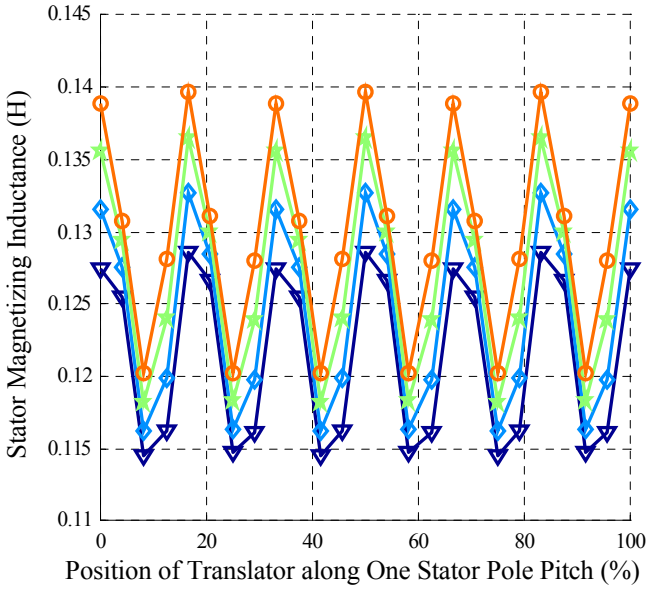

Figure 7. Stator Magnetizing Inductance Variation from FEA

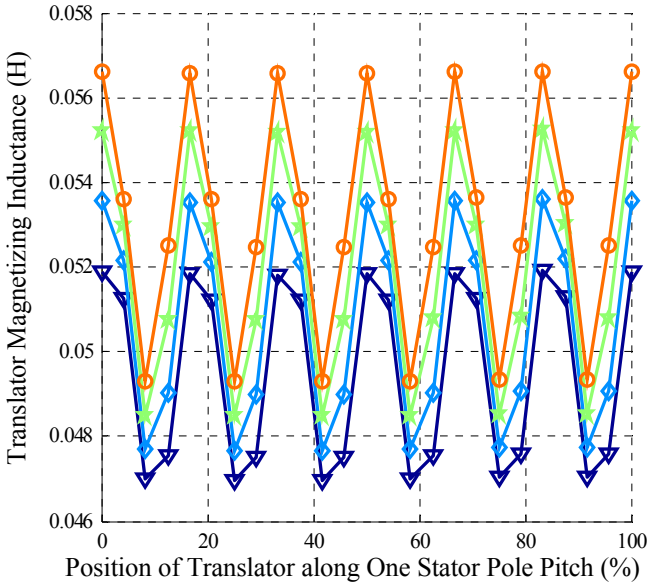

Figure 8. Translator Magnetizing Inductance Variation from FEA

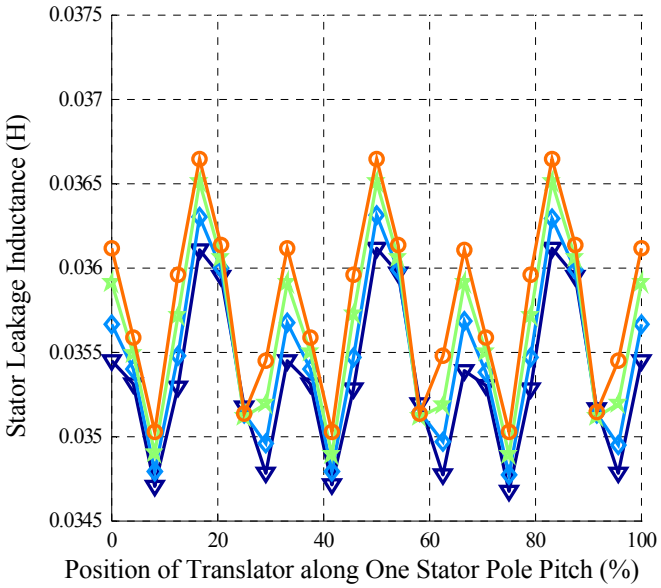

Figure 9. Stator Leakage Inductance Variation from FEA

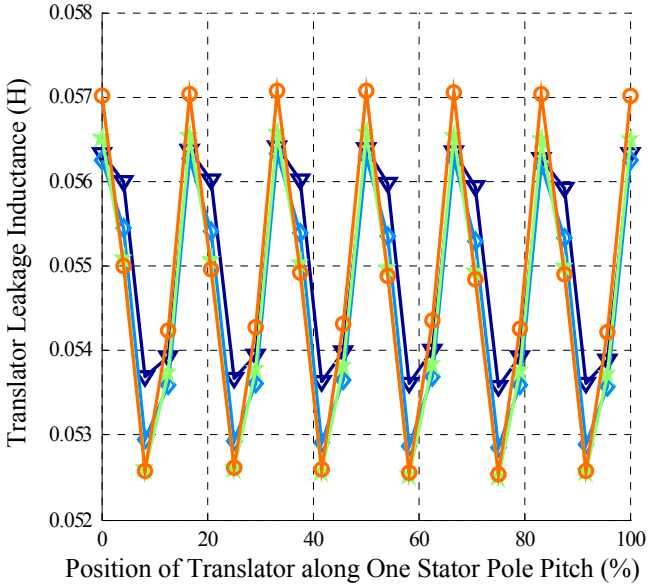

Figure 10. Translator Leakage Inductance Variation from FEA

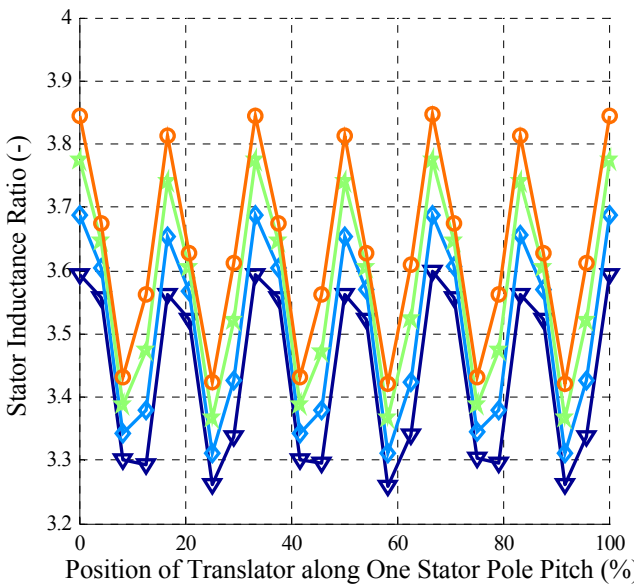

Figure 11. Variation of the Stator Magnetizing to Leakage Inductance Ratio from FEA

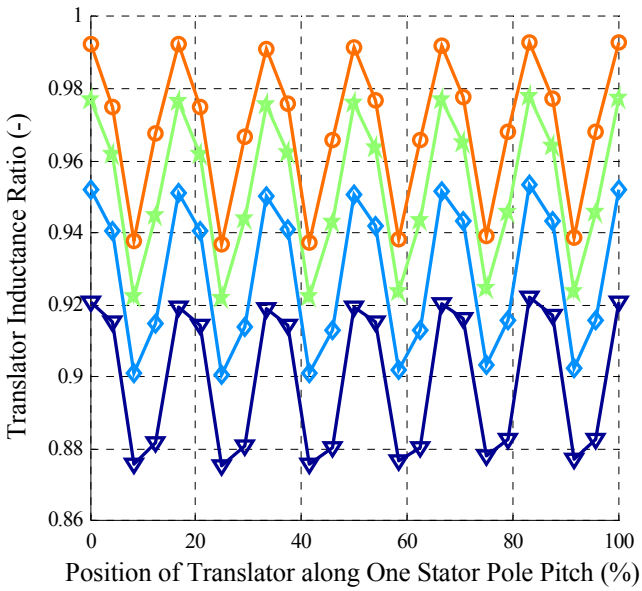

Figure 12. Variation of the Translator Magnetizing to Leakage Inductance Ratio from FEA

2) Ripple Force Calculations and Optimization

Ripple force is the force component in the direction of motion. This type of static force calculation is taken from JMAG when all phases of either the stator or translator are excited. Exciting the stator yields stator ripple force, and exciting the translator yields translator ripple force.

Ripple force profiles for the stator and translator are given in Figs. 14 and 13 respectively. These figures show that the ripple force varies periodically in the same way that the inductance varies. The desired model has the least amount of ripple force.

3) Overview of Optimization Criteria and Choice of Machine Model

Table II presents the four optimization criteria. To recap, we are looking for the model with the least amount of ripple force variation and the largest inductance ratio. It is apparent that the optimization of each parameter is inversely related in that the inductance ratio becomes better as r_{ts} increases while ripple force variation becomes worse.

We can see in Table II that stator ripple force variation starts to drop as r_{ts} reaches 0.675 even as translator ripple force variation still increases. This result bolsters the decision to select r_{ts} = 0.675 as the most desirable model. Table III presents the machine parameters for this model.

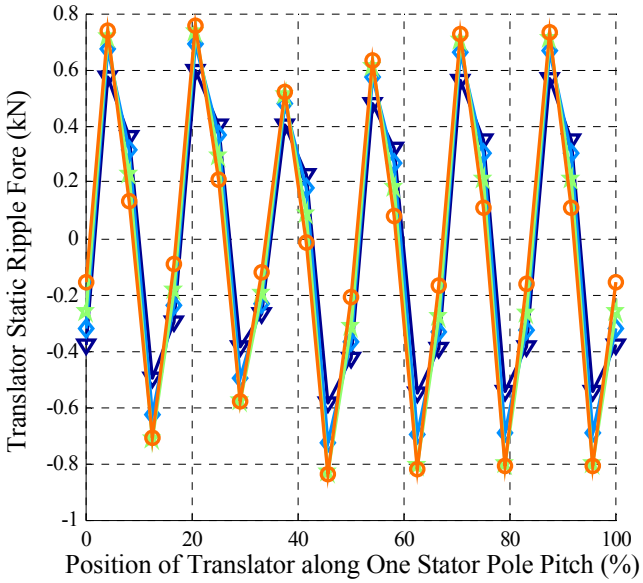

Figure 13. Translator Ripple Force Variation from FEA

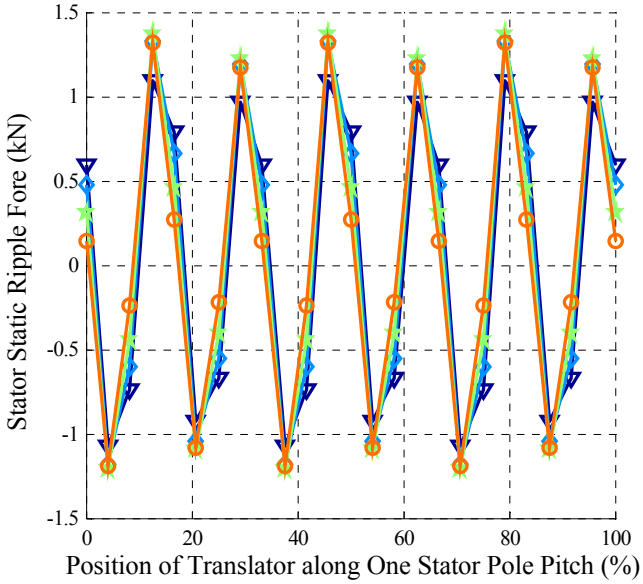

Figure 14. Stator Ripple Force Variation from FEA

TABLE II. FEA OPTIMIZATION CRITERIA

Optimization Criteria		Translator Tip to Slot Pitch Ratio			
		r_{ts} = 0.6	r_{ts} = 0.625	r_{ts} = 0.65	r_{ts} = 0.675
Inductance Ratio (-)	Stator	3.44	3.505	3.572	3.632
	Translator	0.899	0.928	0.953	0.969
Ripple Force Variation (kN)	Stator	1.08	1.26	1.29	1.27
	Translator	0.593	0.709	0.783	0.797

TABLE III. MACHINE PARAMETERS FOR THE r_{ts} = 0.675 MODEL

Parameter	Symbol	Value	Units
Rated Line-Line Voltage	$V_{RMS,LL}$	230	(V_{RMS})
RMS Current	I_{RMS}	14.38	(A)
Maximum Flux Density	B_{max}	2	(T)
Average Airgap Magnetic Flux Density	$B_{g,ave}$	0.46	(T)
Stator coil pitching	$\tau_{s,coil}$	5/6	(-)
Electrical Frequency	ω_{elec}	28.2	(rad/s)
Number of Poles	P	8	(-)
Series stator coil turns per phase	$N_{s,series}$	1205	(turns)
Series translator coil turns per phase	$N_{r,series}$	1124	(turns)
Stator Resistance	$R_{s,1\phi}$	2.8	(Ω)
Translator Resistance	$R_{r,1\phi}$	2.4	(Ω)
Stator slots per pole per phase	q_s	2	(-)
Translator slots per pole per phase	q_r	1	(-)

V. CONCLUSIONS

In this paper, a new type of linear machine topology is presented for use as a direct-drive generator in a buoy-type WEC. While many of the machines being studied for this application conform to the adaptation of permanent magnet machines, this paper explores a new topology. As Laithwaite says, "Get yourself a new shape of motor – find out what it can do" [13]. The proposed hybrid machine combines the superior magnetic coupling of the longitudinal flux machine with the improved force density of the transverse flux machine. An FEA analysis is carried out to validate and optimize the analytical design. FEA validation shows agreement with analytical calculations, and the optimization process results in the r_{ts} = 0.675 model having the best magnetic coupling and ripple force variation characteristics.

Future publications will present experimental results and candidate control algorithms for this machine.

ACKNOWLEDGMENT

The authors would like to thank WEMPEC for their continued support of this research. The expertise and guidance of all those involved in the WEMPEC research group has been greatly appreciated.

REFERENCES

[1] H. Polinder, B.C. Mecrow, A.G. Jack, P.G. Dickinson, and M.A. Mueller, "Conventional and TFPM Linear Generators for Direct-Drive Wave Energy Conversion," IEEE Transactions on Energy Conversion, vol. 20, no. 2, June 2005.

[2] P. Cancelliere, F. Marignetti, V. Delli Colli, R. Di Stefano, and M. Scarano, "A Tubular Generator for Marine Energy Direct Drive Applications," IEEE International Conference on Electric Machines and Drives, pp. 1473-1478, 15-18 May 2005.

[3] N.J. Baker, M.A. Mueller, and E. Spooner, "Permanent Magnet Air-Cored Tubular Linear Generator for Marine Energy Converters", Second

International Conference on Power Electronics, Machines, and Drives, vol. 2, pp. 862-867, 31 Mar. - 2 Apr. 2004.

[4] H. Arof, A.M. Eid, and K.M. Nor, "Permanent Magnet Linear Generator Design Using Finite Element Method," International Conference on Electrical, Electronic and Computer Engineering, pp. 893-896, 5-7 Sept. 2004.

[5] I.A. Ivanova, O. Ågren, H. Bernhoff, and M. Leijon, "Simulation of Cogging in a 100kW Permanent Magnet Octagonal Linear Generator for Ocean Wave Conversion," International Symposium on Underwater Technology, pp. 345-348, 20-23 Apr. 2004.

[6] H. Arof, A.M. Eid, and K.M. Nor, "Cogging Force Reduction Using Special Magnet Design for Tubular Permanent Magnet Linear Generators," 39th International Universities Power Engineering Conference, vol. 1, pp. 523-527, 6-8 Sept. 2004.

[7] P.L. Jansen, "The Integration of State Estimation, Control, and Design for Induction Machines," Ph.D. dissertation, University of Wisconsin-Madison, 1993.

[8] E.R. Laithwaite, Linear Electric Motors, London, UK: Mills & Boon Limited, 1971.

[9] M. Poloujadoff, The Theory of Linear Induction Machinery, Thetford, UK: Oxford University Press, 1980.

[10] J.K. Dukowicz, "Analysis of Linear Induction Machines with Discrete Windings and Finite Iron Length," IEEE Transactions on Power Apparatus and Systems, vol. PAS-96, no. 1, Jan./Feb. 1977.

[11] I.A. Ivanova, O. Ågren, H. Bernhoff, and M. Leijon, "Simulation of Wave-Energy Converter with Octagonal Linear Generator," IEEE Journal of Oceanic Engineering, vol. 30, no. 3, July 2005.

[12] T.A. Lipo, Introduction to AC Machine Design, 2nd ed., WisPERC, 2004.

[13] E.R. Laithwaite, "Linear Electric Machines – A Personal View," Proceedings of the IEEE, vol. 3, no. 2, pp. 250-315, Feb. 1975.